

2009

Electrostatically Tunable Analog Single Crystal Silicon Fringing-Field MEMS Varactors

Joshua A. Small

Purdue University - Main Campus, jsmall03@purdue.edu

Xiaoguang Liu

Purdue University - Main Campus, liu79@purdue.edu

Anurag Garg

Purdue University - Main Campus, garg@purdue.edu

Dimitrios Peroulis

Birck Nanotechnology Center and School of Electrical and Computer Engineering, Purdue University, dperouli@purdue.edu

Follow this and additional works at: <http://docs.lib.purdue.edu/nanopub>



Part of the [Nanoscience and Nanotechnology Commons](#)

Small, Joshua A.; Liu, Xiaoguang; Garg, Anurag; and Peroulis, Dimitrios, "Electrostatically Tunable Analog Single Crystal Silicon Fringing-Field MEMS Varactors" (2009). *Birck and NCN Publications*. Paper 551.
<http://docs.lib.purdue.edu/nanopub/551>

This document has been made available through Purdue e-Pubs, a service of the Purdue University Libraries. Please contact epubs@purdue.edu for additional information.

Electrostatically Tunable Analog Single Crystal Silicon Fringing-Field MEMS Varactors

Joshua Small, Xiaoguang Liu, Anurag Garg and Dimitrios Peroulis

Birck Nanotechnology Center, School of Electrical and Computer Engineering, Purdue University
West Lafayette, IN 47906 United States of America

smallj@purdue.edu
liu79@purdue.edu
garg@purdue.edu
dperouli@purdue.edu

Abstract—This paper reports on the design of a new analog MEMS varactor that uses electrostatic fringing-field actuation and is based on a single-crystal silicon movable structure coated with a thin metallic layer. Electrostatic fringing-field actuation allows for an analog displacement with no pull-in instability that yields a much larger tuning ratio compared to conventional electrostatic designs. In addition, total lack of dielectric layers and the use of single crystal silicon for the moving membrane significantly enhances the robustness of our proposed varactor by making it devoid of dielectric charging and stiction, insensitive to process variations, amenable to high yield manufacturing and less susceptible to hysteresis and creep. Based on this idea, we present example designs and the associated fabrication processes for varactors that exhibit a tuning ratio of 4.5:1 with capacitance values in the range of 43-200 fF achieved with DC voltages of 0-55 V. Such varactors are key elements in MEMS matching networks, tunable filters and reconfigurable antennas in the K/Ka/W-bands.

Index Terms—Electrostatic devices, microelectromechanical devices, silicon on insulator technology, tuning, tunable circuits and devices, varactors.

I. INTRODUCTION

Radio Frequency (RF) Micro-Electro-Mechanical systems (MEMS) tunable varactors have been designed and developed for a variety of high frequency communication systems [1]. Tunable varactors are important components in subsystems such as oscillators, tunable filters and tunable matching networks to name a few [1-5]. The most popular technologies for building MEMS varactors are the analog parallel plate approach [3] the analog interdigital design [2] and a digital capacitance bank using MEMS switches [4]. Analog varactors offer stiction-free performance, but are limited by the pull-in phenomenon and creep/viscoelasticity. Digital varactors, on the other hand, exhibit higher tuning range, stability and immunity to noise at the cost of dielectric charging, stiction and lower quality factors.

This paper proposes a varactor that employs the fringing-field actuation approach along with parallel plate capacitive tuning. Electrostatic fringing field actuation preserves the key benefits of parallel plate actuation while also increasing the robustness and reliability of the device design by completely eliminating dielectric layers and providing stable and contactless operation over the entire gap without using special

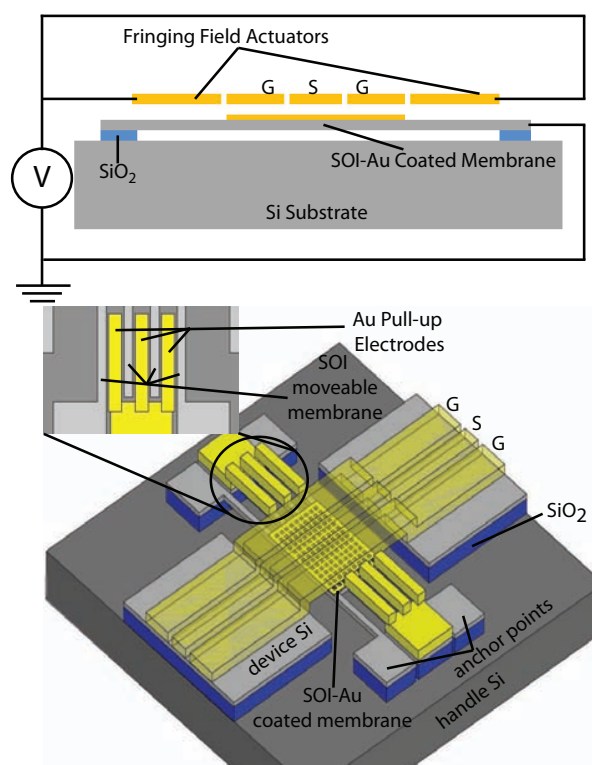


Fig. 1. Side view and three-dimensional schematic of the proposed fringing field actuated MEMS varactor.

biasing techniques and complex device configurations. The proposed varactor is manufactured as a composite of gold and single-crystal silicon for the movable membrane. Incorporating single-crystal silicon as part of the structural layer for the movable membrane improves the robustness of the device by allowing it to be less susceptible to hysteresis, creep and thin film post-release residual stress [6], [7]. Lastly, the actuation mechanism is completely decoupled from the RF lines. Such decoupling has been demonstrated to improve the RF performance of MEMS varactors [5].

II. DESIGN

Fig. 1 shows a schematic of the proposed varactor. This device is implemented as a capacitive shunt coplanar waveguide (cpw) topology. The transmission line in this example is a 50/60/50 μm cpw line. As fig. 1 illustrates, the cpw, movable bridge and pull up fringing field electrodes are released. Unlike typical shunt capacitive designs where the movable membrane is the top most layer and the cpw line is fixed to the substrate, this design has a 20- μm low stress electroplated fixed Au cpw line suspended 3- μm over a movable 5- μm thick, fixed-fixed flexure, capacitive shunt membrane (lower beam). This inverted implementation is chosen for compatibility with the Silicon-On-Insulator (SOI) processing described in Section III. The fixed-fixed flexure anchoring is chosen to reduce the spring constant and to permit access to the pull up electrodes for biasing. The pull up fringing field electrodes are also suspended above the movable bridge and are laterally offset in a combdrive configuration throughout the width of the movable beam. The lateral separation between the pull-up electrode teeth and the SOI-Au coated membrane teeth is 5- μm . This gap distance is a reasonable compromise between acutation voltage and practical fabrication tolerances and limitations. The pull up electrodes are electroplated in the same process step as the cpw line to a thickness of 20- μm with a length of 450- μm along the length of the movable membrane body, beginning at the anchor points. This thickness of Au is chosen to permit robust processing, ensuring no possibility of membrane collapse during the release and critical point drying process. It is also important to mention that the Au coating on the SOI membrane does not extend all the way to the anchor points. Thus the anchor points of the movable structure, which face the maximum stress, are composed entirely of single-crystal silicon. This is critical in order to ensure minimum sensitivity to creep and viscoelasticity. Table 1 summarizes the physical and material parameters of the proposed varactor.

When a potential difference is applied between the fringing field electrodes and the MEMS SOI membrane, a stable and linear deflection of the lower membrane throughout the entire gap is achieved. The combdrive configuration of the fringing field pull-up electrodes serves to increase the electrostatic fringing field force by a multiple that is directly proportional to the number of interdigital fingers. The proposed design successfully couples the high absolute capacitance of the parallel plate approach with the wide tuning range of the interdigital approach.

III. FABRICATION

Fig. 2 summarizes the four-mask process that is necessary for the fabrication of the varactor. The varactor is fabricated on a high-resistivity SOI substrate; with a device layer resistivity of approximately 3000 $\Omega\text{-cm}$ and thickness of 2- μm , a buried oxide thickness of 4- μm , and a handle resistivity of 3000 $\Omega\text{-cm}$ and thickness of 500- μm . The fabrication starts with deposition and wet etch patterning of Cr/Au 300/5000 \AA to define the metallic trace to vary the shunt capacitance, anchors for suspended structures and probe pads. Next, the silicon

TABLE I
TYPICAL DIMENSIONS AND MATERIAL PARAMETERS OF ELECTROSTATIC FRINGING FIELD ACTUATOR

Parameter	Value
Beam length	1500 μm
Beam width	200 μm
Beam thickness	5 μm
Release hole ligament efficiency	0.5
Fringing Field Pull-up electrode spacing	5 μm
Pull-up electrode vertical gap	4 μm
Au Young's Modulus	78 GPa
Au Poisson Ratio	0.44
Si Young's Modulus	129.5 GPa
Si Poisson Ratio	0.28

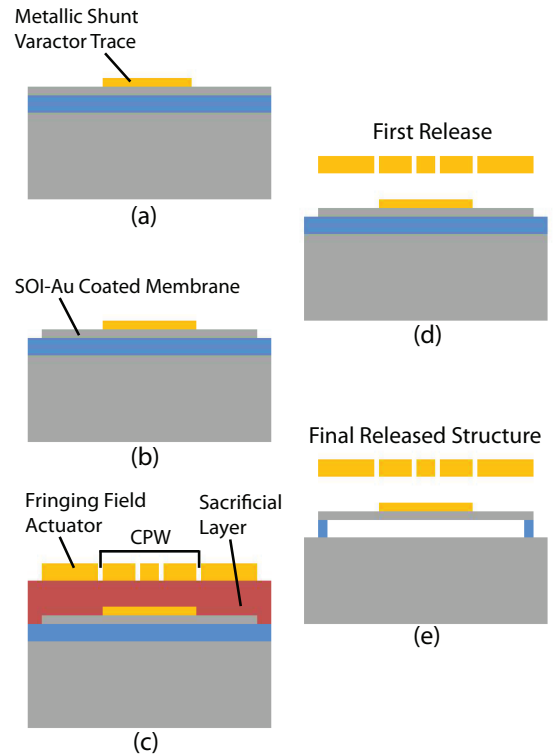


Fig. 2. Process flow of proposed fringing field actuated MEMS varactor.

device layer is patterned and reactive ion etched using SF_6 plasma to form the SOI movable membrane and electrical isolation between the actuation electrodes, the cpw and the MEMS tuner. The photoresist sacrificial layer (SC1827 by Shipley) is subsequently spun at 3.5 krpm and patterned. This sacrificial layer is post-baked at 170 $^\circ\text{C}$ on a hotplate for 3 minutes to avoid any out-gassing in the remaining process. A seed layer of Cr/Au 300/1000 \AA is sputter deposited on top of the sacrificial layer. This layer is electroplated to 20- μm to create the very stiff suspended cpw lines and fringing field actuators as described in Section II. The final steps are etching the sacrificial photoresist and buried oxide layers to release the cpw lines, fringing field pull up electrodes and the SOI Au coated membrane and critical point drying.

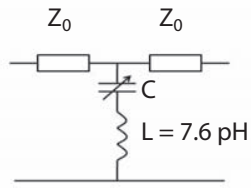


Fig. 3. Equivalent circuit used to extract capacitance values vs. bias voltage.

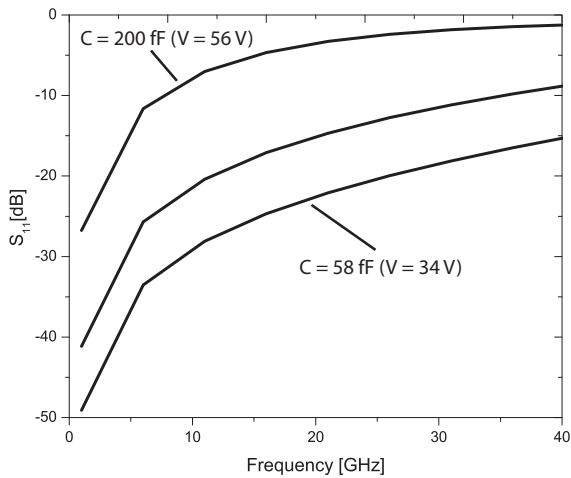


Fig. 4. Simulated reflection coefficient of proposed varactor.

IV. RESULTS AND DISCUSSION

A. Tuning Range

Fig. 3 and 4 shows the equivalent circuit and simulated reflection coefficient for the proposed varactor, respectively. Fig. 5 shows the simulated shunt capacitance of the fringing field varactor. The capacitance simulation was performed with boundary element method in CoventorWare with the parameters listed in Table 1. Residual mean stress due to the deposited gold is not included in the simulation due to the designed rigid nature of the movable SOI membrane and the absence of deposited gold on the primary actuation beams near the anchors. Fig. 6 illustrates the deflection vs. applied bias for the fringing field actuated MEMS tuner and as before, performed with the electromechanical simulator in CoventorWare. Fig. 7 presents the expected beam profile as a function of applied bias. The image is exaggerated in the z-direction to better illustrate the beam deflection. The varactor demonstrates a total practical tuning of 4.5:1 for capacitances of 43-200 fF under a bias voltage of 0-55 V. Voltages beyond 55 V were not included because the gap reduces to less than $0.5\text{-}\mu\text{m}$ which proves difficult to achieve in practice. Therefore, with a capacitance of 200 fF we are taking a conservative

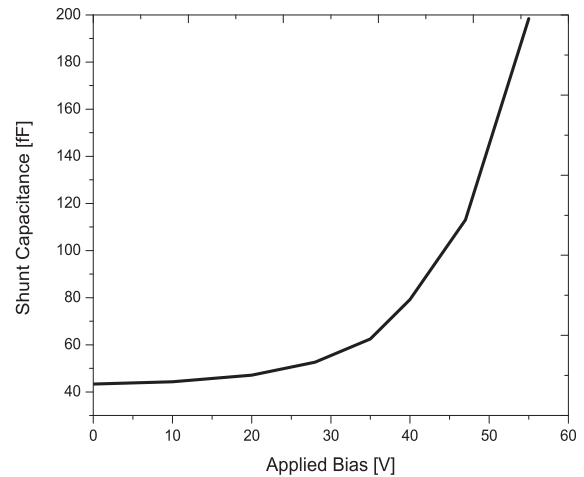


Fig. 5. Shunt capacitance as a function of applied bias voltage.

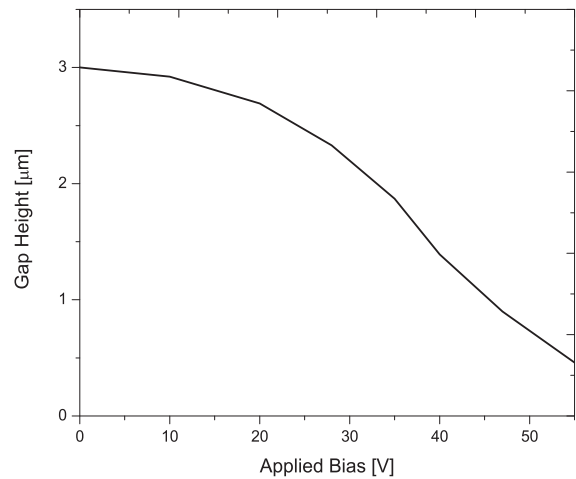


Fig. 6. Electromechanical simulation of expected deflection as a function of applied bias voltage for the proposed varactor.

stance, estimating maximum varactor control to a gap of $0.5\text{-}\mu\text{m}$. From the simulated performance, we expect the tuner to provide stable control throughout the entire gap as described in Section II and demonstrated by fig. 6. The primary reason for this stability is the perpetual equilibrium of the electrostatic and mechanical forces as the gap reduces. In typical parallel plate electrostatic designs, the electrostatic force is highly non-linear as the gap reduces, limiting the stable equilibrium region to a small interval of the total gap.

B. Electrostatic Fringing Field Force

Fig. 8 illustrates electrostatic fringing field force as a function of pull-up electrode quantity. A linear relationship in the force as the electrode quantity increases is observed. This phenomena has been well studied and modeled in combdrive electrostatic actuators. And just as in combdrive actuators, large and continuous deflection throughout the entire travel range can be expected from electrostatic fringing field actuators.

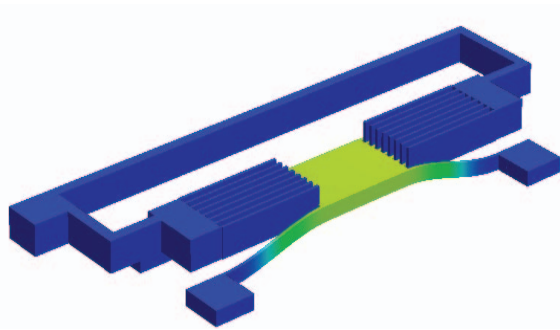


Fig. 7. CoventorWare snap shot of beam profile as a function of applied bias voltage for proposed varactor.

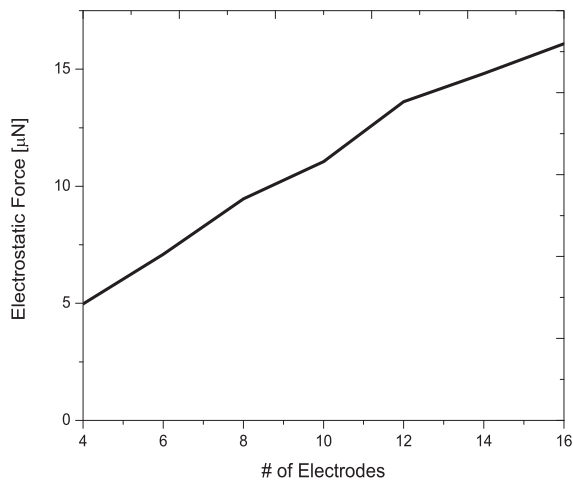


Fig. 8. Electrostatic fringing field force versus number of combdrive pull-up electrodes for beams with dimensions listed in table 1.

C. Electromagnetic Resonant Frequency and Quality Factor

The resonant frequency of the design is dominated by the highest capacitance value and the parasitic inductance. The parasitic inductance depends strongly on the geometry of the springs for the SOI Au coated membrane. In our design, the movable beam shunt plate is a continuous sheet, with no special anchoring to the ground planes. Based on simulations with the equivalent circuit of fig. 3, this brings our parasitic inductance in the order of 7 pH [1]. For practical gaps as described in the previous subsection, this brings our resonant frequency to over 100 GHz. The quality factor is anticipated to be very high due to the thick cpw lines used in our design. In addition, as mentioned in the introduction, decoupling the actuation and the cpw lines also provides a boost in RF performance due to the reduced interaction of the DC and RF lines.

V. CONCLUSION

A new electrostatic analog fringing field actuated MEMS varactor is presented in this paper. The achieved capacitances are from 43-200 fF with an applied bias of 0-55 V. This results in a wide tuning range of 4.5:1. The proposed MEMS varactor combines the compact and high absolute capacitance

of parallel plate structures with the wide tuning range and stable deflection of interdigital actuators.

ACKNOWLEDGEMENT

This work has been supported by the Defense Advanced Research Projects Agency under the IMPACT Program grant No. 2006-05822-06. The authors wish to acknowledge the assistance and support of Shoaib Arif, Adam Fruehling, and Nithin Raghunathan. As well as the support of the Birck Nanotechnology Center technical staff.

REFERENCES

- [1] G. Rebiez, "RF MEMS: Theory, Design and Technology" *John Wiley and Sons*, 2003.
- [2] J.J. Yao, S. Park, and DeNatale, "High Tuning Ratio MEMS-based Tunable Capacitors for RF Communications Applications" *Solid State Sensors and Actuators Workshop*, pp. 124-127, 1998.
- [3] J. Zou, C. Liu, and J. Schutt-Aine, "Development of a Wide Tuning-range Two-parallel-plate Tunable Capacitor for Integrated Wireless Communication Systems" *Int. J. RF and Microwave CAE*, vol.11, pp. 322-329, 2001.
- [4] C. L. Goldsmith, A. Malczewski, Z. J. Yao, S. Chen, J. Ehmke, and D. H. Hinzl, "RF MEMS Variable Capacitors for Tunable Filters," *Int. J. RF and Microwave CAE*, vol. 9, pp. 362-374, July 1999.
- [5] X. Liu, L.P.B. Katehi, W.J. Chappell, D. Peroulis, "A 3.4 - 6.2 GHz Continuously Tunable Electrostatic MEMS Resonator with Quality Factor of 460-530" *2009 IEEE MTT-S Int. Microwave Symp. Dig.*, in print.
- [6] A. Fruehling, D. Peroulis, "A Single-crystal Silicon DC-40 GHz RF MEMS Switch" *2009 IEEE MTT-S Int. Microwave Symp. Dig.*, in print.
- [7] D. Vickers-Kirby et al., "Anelastic Creep Phenomena in thin film Metal Plated Cantilevers for MEMS", *Materials Science of MEMS Devices*, vol. 657, p. EE2.5.1-2.5.6, 2001.
- [8] D. Peroulis, L. P. B. Katehi, "Electrostatically-Tunable Analog RF MEMS Varactors with Measured Capacitance Range of 300%" *2003 IEEE MTT-S Int. Microwave Symp. Dig.*, vol. 3, pp. 1793-1796.
- [9] High Frequency Structural Solver, Ansoft Corporation, <http://www.ansoft.com/products/hf/hfss>
- [10] CoventorWare, <http://www.coventor.com>